HHS Public Access

Author manuscript

Nat Chem. Author manuscript; available in PMC 2020 May 01.

Published in final edited form as:

Nat Chem. 2019 November ; 11(11): 987–993. doi:10.1038/s41557-019-0343-5.

An enzymatic platform for the asymmetric amination of primary, secondary and tertiary C(sp³)-H bonds

Yang Yang[1], **Inha Cho**[1], **Xiaotian Qi**[2], **Peng Liu**[2,*], **Frances H. Arnold**[1,*]

[1]Division of Chemistry and Chemical Engineering, California Institute of Technology, Pasadena, California 91125, USA.

[2]Department of Chemistry, University of Pittsburgh, Pittsburgh, Pennsylvania 15260, USA.

Summary

The ability to selectively functionalize ubiquitous C–H bonds streamlines the construction of complex molecular architectures from simple and easily available precursors.[1–3] Despite recent advances with small-molecule catalysts based on transition metals, C(sp^3)–H bonds still present considerable hurdles for stereoselective modification.[4,5] Here we describe enzyme catalysts derived from a cytochrome P450 that use a nitrene transfer mechanism for the enantioselective amination of primary, secondary, and tertiary C(sp^3)–H bonds. These fully genetically encoded enzymes are produced and function in bacteria, where they can be optimized by directed evolution for a broad spectrum of enantioselective C(sp^3)–H amination reactions. These catalysts can aminate a variety of benzylic, allylic, and unactivated aliphatic C–H bonds in excellent enantioselectivity with access to either antipode of product. Additionally, enzyme-catalysed enantioselective amination of primary C(sp^3)–H bonds in substrates bearing geminal dimethyl substituents furnished chiral amines featuring an all-carbon quaternary stereocentre.[6] Moreover, these enzymes enabled the enantioconvergent transformation[7] of racemic substrates possessing a tertiary C(sp^3)–H bond to afford products bearing a tetrasubstituted stereocentre, a process that has eluded small molecule catalysts. Further engineering allowed for the enantioselective construction of 'methyl (Me) - ethyl (Et)' stereocentres (87% enantiomeric excess), which is notoriously challenging in asymmetric catalysis due to the minimal spatial and chemical differentiation of these substituents.[8] Total turnover numbers (TTNs) of up to 72,000 have been achieved. The ability of these iron-based catalysts to facilitate the enantioselective functionalization of all three types of C(sp^3)–H bonds in abiological transformations is expected to inspire novel asymmetric transformations in chemistry and synthetic biology.

*Correspondence should be addressed to F.H.A. (frances@cheme.caltech.edu) and P.L. (pengliu@pitt.edu).

Author contributions

Y.Y. designed the overall research with F.H.A. providing guidance. Y.Y. and I.C. designed and performed the initial screening of heme proteins and directed evolution experiments. Y.Y. designed and performed the substrate scope study and mechanistic study. X.Q. carried out the computational studies with P.L. providing guidance. Y.Y. and F.H.A. wrote the manuscript with the input of all other authors.

Data and materials availability: All data are available in the main text and the Supplementary Materials. Solid-state structures of **2a**, **4a**, **5a** and **5f** are available free of charge from the Cambridge Crystallographic Data Centre under reference numbers CCDC 1905551, 1905553, 1905552 and 1905554. Plasmids encoding the enzymes reported in this study are available for research purposes from F.H.A. under a material transfer agreement with the California Institute of Technology.

Author Information

A provisional patent application has been filed through the California Institute of Technology based on the results presented here.

The development of general systems for the highly enantioselective transformation of C(sp^3)–H bonds lies at the forefront of current efforts to advance transition-metal-catalysed C–H functionalization.[4] In principle, several classes of enantioselective C(sp^3)–H functionalization can be developed, depending on the topicity and degree of substitution (primary, secondary, or tertiary) of the sp^3-hybridized carbon atom undergoing functionalization (Fig. 1). As depicted in Fig. 1a, effective enantiodiscrimination of the two prochiral secondary C(sp^3)–H bonds at a methylene unit leads to the formation of a trisubstituted stereogenic centre.[4] On the other hand, asymmetric primary C(sp^3)–H functionalization by differentiating the two prochiral methyl substituents can serve as a powerful means to access challenging all-carbon quaternary stereocentres (Fig. 1b).[4,9] As a distinct alternative, the enantioselective functionalization of a tertiary C(sp^3)–H bond will enable the conversion of readily available precursors into valuable products featuring a tetrasubstituted stereocentre (Fig. 1c). Due to the presence of a pre-existing stereogenic centre at the site of attachment, this process would require the enantioconvergent functionalization[7] of a tertiary C(sp^3)–H bond to convert both enantiomers of the racemic substrate into the same major enantiomer, a daunting challenge that so far remains out of the reach of small-molecule transition-metal catalysts. In this context, identifying a set of structurally related catalysts as a unified platform for the asymmetric functionalization of all three types of aliphatic C–H bonds will accelerate further development and application of C–H functionalization technologies.

Enabled by numerous potentially cooperative protein-substrate interactions within the elaborate chiral scaffold of the active site, enzymes can exert exquisite control over the stereochemical outcome of various catalytic reactions, including C–H functionalization.[10] Among naturally occurring enzymatic C–H functionalization processes, cytochrome P450-catalysed C(sp^3)–H hydroxylation represents a venerable example of outstanding stereocontrol.[11,12] Over the past six years, our laboratory[13,14] and others[15–18] have repurposed these enzymes and other heme proteins to catalyse synthetically useful reactions that are not known to nature. In particular, we have engineered heme proteins for abiological C–H functionalization leading to the formation of C–C and C–N bonds via a carbene[19] or nitrene[20–22] transfer mechanism. Collectively, these results showcase enzymes' potential for performing abiological asymmetric C–H functionalization reactions, using earth-abundant iron in a fully genetically-encodable protein that can be tuned by evolution. The capabilities of enzymes to solve key outstanding problems in asymmetric catalysis, however, have not yet been tested in these C–H functionalization processes.

Herein, we describe the development of general cytochrome P450-based biocatalysts for the asymmetric amination of primary, secondary and tertiary C(sp^3)–H bonds in the synthesis of chiral diamines, a key pharmacophore in numerous antiviral and antibacterial agents (Fig. 1d and Supplementary Information Fig. S1).[23,24] Inspired by the pioneering work of other groups in the area of transition-metal-catalysed intramolecular C(sp^3)–H amination[3,5,25–31]as well as our own studies[20–22], we envisioned a unified enzymatic strategy for the catalytic asymmetric assembly of diverse 1,2- and 1,3-diamines from abundant amine precursors. As outlined in Fig. 1d, using a previously established one-step procedure,[24] the aliphatic amine (**I**) can be readily converted to the corresponding sulfamoyl

azide (**II**) in excellent yield. Our proposed biocatalytic C(sp^3)–H amination would lead to the formation of the enantioenriched cyclic sulfamide (**III**). Subsequent excision of the sulfonyl unit using known procedures[24] would then furnish the desired chiral diamine (**IV**, see the Supplementary Information for details of converting sulfamides to diamines). In addition to its synthetic utility, we postulated that this chiral diamine synthesis could serve as an ideal platform to identify and evolve heme proteins for the asymmetric amination of all three types of C(sp^3)–H bonds (Fig.1a–c), especially those that have not succumbed to small molecule-catalysed asymmetric C–H functionalizations.

We commenced our study by evaluating a panel of heme proteins including variants of cytochromes P450, cytochromes P411 (P450 with the iron coordinating cysteine residue replaced by a serine), cytochromes *c* and globins in intact *Escherichia coli* cells for enantioselective diamine synthesis (Fig. 2a). We focused our initial investigation on the asymmetric synthesis of 1,2-diamine derivatives due to the lack of highly enantioselective C–H amination methods for synthesizing these compounds.[32] Among the heme proteins we tested, a few variants from the cytochrome P450 superfamily showed low levels of C–H amination activity (see Supplementary Information for details). In particular, a truncated P411 variant lacking the FAD domain ($P411_{Diane1}$, P411 diamine synthase), which we developed during an earlier study on Fe-catalysed carbene insertion into C(sp^3)–H bonds,[19] was over 10 times more active than other heme proteins, providing a total turnover number (TTN) of 450 and an enantiomeric excess (ee) of 94% for the 1,2-diamine product (**2a**). This demonstrates that the reductase domain of cytochrome P450 is not needed for C–H amination. Finally, the absolute stereochemistry of **2a** was ascertained by single crystal X-ray diffraction analysis.

We used $P411_{Diane1}$ as the starting template for directed evolution of 1,2-diamine synthase (Fig. 2a). In an effort to further improve the enzyme's activity and enantioselectivity for this C–H amination process, we performed iterative rounds of site-saturation mutagenesis (SSM) and screening, targeting amino acid residues close to the heme cofactor. For each round of engineering, enzyme libraries were expressed and screened in 96-well plates in the form of whole *E. coli* cells. Beneficial mutations I327P, Y263W and Q437F were introduced in three rounds, furnishing a 10-fold improvement in activity as well as further enhancements in enantioselectivity. Notably, undesired nitrenoid reduction was also effectively suppressed. Using final variant $P411_{Diane2}$, the C(sp^3)–H amination product formed in 3490 TTN and 99.9% ee as determined by chiral gas chromatography (GC). Moreover, by further lowering the cell density in whole-cell biotransformations, this enzymatic C–H amination provided the diamine product in 72,000 TTN and 99.9% ee, thereby demonstrating the excellent catalytic efficiency of our engineered P411 enzyme relative to previously developed transition-metal catalysts.

Using *E. coli* whole cells harbouring $P411_{Diane2}$, we surveyed the substrate scope of this C(sp^3)–H amination process for 1,2-diamine synthesis (Fig. 2b). Electron-donating and electron-withdrawing substituents on the aromatic ring were compatible with this process (**2a**–**2g**), affording 1,2-diamines with uniformly high-levels of enantioselectivity. Additionally, substrates bearing a halogen functional group handle for further derivatization were accepted by the enzyme (**2e** and **2f**). Steric hindrance at the *ortho* position was also

compatible (**2h**), although lower activity was observed. Structural perturbations such as replacement of the aryl ring by thiophene (**2i**) and variance of the *N*-substituent (**2j**) were well-tolerated by this biocatalytic C(sp^3)–H amination. Moreover, we found that the starting variant $P411_{Diane1}$ could be employed for the asymmetric synthesis of 1,3-diamine derivatives using C(sp^3)–H amination. In addition to the asymmetric amination of benzylic C(sp^3)–H bonds (**2k**–**2n**), allylic C(sp^3)–H bonds (**2o**) were also effectively aminated with excellent enantioselectivity. In contrast to $Rh(OAc)_2$-based systems,[25] competing aziridination product was not observed, highlighting the chemoselectivity of these iron-based biocatalysts.

Furthermore, directed evolution of $P411_{Diane1}$ furnished a complementary set of enzymatic catalysts allowing for the enantiodivergent amination of unactivated secondary aliphatic C(sp^3)–H bonds (Fig. 2c). Amino acid residue 87 located in a loop in the active site and known for its importance in substrate recognition in P450-catalysed oxidation and carbene transfer reactions[33,34] was found to play a dominant role in determining the sense of absolute stereochemistry of the C–H amination product. Specifically, a single A87I mutation inverted the absolute configuration of the newly formed stereocentre. With this initial result, additional rounds of SSM and screening led to $P411_{Diane1}$ L82M A87I Y263W I327S, delivering the C(sp^3)–H amination product in 96% ee (*R* enantiomer). On the other hand, leaving A87 unchanged, a single mutation I327T resulted in a significant enhancement in enantioselectivity (32% ee to 71% ee). This is a rare example of enantiodivergent C(sp^3)–H amination reactions catalysed by engineered heme proteins.

Having engineered a set of enzymes for the asymmetric amination of secondary C(sp^3)–H bonds, we questioned whether this enantioselective amination could be extended to the conversion of unactivated primary aliphatic C(sp^3)–H bonds, a thermodynamically more challenging process.[27] Examination of our $P411_{Diane}$ collection revealed that the $P411_{Diane1}$ I327P variant already displayed excellent activity and enantioselectivity for the aminative desymmetrization of geminal dimethyl substituents, providing the desired 1,3-diamine possessing an all-carbon quaternary stereocentre at the β position in 99% ee (Fig. 3a). In the realm of asymmetric catalysis, the desymmetrization of geminal dimethyl groups has been recognized as a promising solution to bypass the long-standing problem of enantioselective methylation.[35] In this context, our biocatalytic desymmetrization represents a valuable example of C–N bond formation for the construction of methyl-substituted stereocentres. Subsequent examination of substrate scope revealed that this desymmetrization is also applicable to other substrates bearing various aryl groups (**4a**–**4d**). The absolute configuration of **4a** was determined by X-ray diffraction analysis.

The enantioselective functionalization of tertiary C(sp^3)–H bonds found in racemic substrates represents an unsolved problem for small molecule catalysts. In particular, enantioconvergent protocols to transform both antipodes of the racemic C–H substrate into the same major enantiomer of the product remain elusive, although conceptually similar enantioconvergent transformations of tertiary alkyl halides have recently received considerable attention.[36–38] Previous studies indicated that iron nitrene-mediated C–H amination may involve a radical mechanism,[39,40] thus suggesting the possibility of achieving stereochemical convergence in the enzymatic tertiary C(sp^3)–H functionalization.

Nonetheless, such enzymatic enantioconvergent transformations would require the same heme protein to accommodate both antipodes of the racemic substrate, a process rarely found in nature's biochemical repertoire. To our delight, we found that $P411_{Diane1}$ could effect the enantioconvergent C(sp^3)–H amination to provide diamine product **5a** featuring a tetrasubstituted stereocentre (99% ee). Iterative SSM and screening generated improved variant $P411_{Diane3}$. Bearing beneficial mutations L78A, A87G, Q437G and I327V, $P411_{Diane3}$ provided the diamine product in 76% yield, 1910 TTN and 99% ee. More importantly, $P411_{Diane3}$ was found to be effective in the enantioconvergent amination of other substrates (**5a**–**5f**). Electron-donating (**5b**), electron-withdrawing (**5c**) and *ortho*-substituents (**5d**) were effectively tolerated under these conditions. Substrates bearing heterocycles (**5e**) and other branching alkyl groups (**5f**) could also be transformed with excellent enantioselectivity.

The effective discrimination between two minimally differentiated methyl- (Me-) and ethyl- (Et-) groups to construct 'methyl-ethyl' stereocentres is a notoriously difficult problem in asymmetric catalysis.[8,41] We envisioned that engineered heme proteins could provide a powerful platform to address this challenge. Indeed, directed evolution of $P411_{Diane1}$ led to $P411_{Diane4}$ bearing five additional mutations (L82C, L181V, I327T, A330M and Q437G), culminating in the enantioconvergent formation of 'methyl-ethyl' stereocentre (**5g**) in 82% yield, 2120 TTN and 87% ee. This result represents a rare example of solving the 'methyl-ethyl' problem using a C(sp^3)–H functionalization strategy.

Mechanistic and computational investigations provided further insight into this enantioconvergent C(sp^3)–H amination process. First, we prepared sulfamoyl azide substrates bearing a stereochemically well-defined olefin moiety ((*Z*)-**1d** and (*E*)-**1d**) and subjected them to the enzymatic reactions. Partial scrambling of the olefin geometry was observed in both the (*E*)- and (*Z*)-substrates, with the (*Z*)-substrate providing a substantial amount of the scrambled product bearing a thermodynamically more stable (*E*)-olefin. The erosion of C=C double bond stereochemistry is consistent with the formation of a carbon-centred radical at the allylic position and does not agree with a concerted C–H insertion mechanism. Consistent with literature reports on related iron-based catalyst systems,[39,40,42] these findings support a radical mechanism for this cytochrome P450-catalysed C(sp^3)–H amination process. Thus, we postulate that this enantioconvergent amination comprises a stereoablative hydrogen atom transfer (HAT) and an enantioselective C–N bond formation. As described in Fig. 4b, reaction of the ferrous heme cofactor with the racemic azide substrate leads to an open-shell Fe-nitrenoid intermediate. Subsequent stereoablative HAT results in the formation of a carbon-centred radical, which then undergoes the final radical rebound step with high levels of enantioselectivity. This mechanistic proposal is further corroborated by our DFT calculations. Computational studies (Fig. 4c) on an iron porphyrin model system showed that the triplet state of the key Fe-nitrenoid intermediate **7** is 3.0 kcal/mol more stable than the open-shell singlet state and 11.6 kcal/mol more stable than the quintet state (see Supplementary Information for the comparison between open-shell singlet, triplet, and quintet free energy profiles). The calculated Mulliken spin density of **7** revealed a spin density of 0.84 on the N atom and 1.16 on the Fe atom, demonstrating significant radical characters on both the nitrogen and the iron centre. In addition, our computations

suggest that the hydrogen atom transfer is irreversible and occurs through triplet transition state **TS1** with an energy barrier of 15.7 kcal/mol (Fig. 4c). Furthermore, the subsequent radical rebound step proceeding through quintet transition state **TS2** requires an activation energy of 18.4 kcal/mol, suggesting sufficient lifetime of the carbon-centred radical to allow for stereoablation and the subsequent enantioselective C–N bond formation observed in the enzymatic reaction.

In conclusion, we have developed a biocatalytic platform for the asymmetric amination of a variety of C(sp^3)–H bonds, permitting a diverse range of synthetically useful chiral diamines to be prepared with excellent enantioselectivity. These biocatalysts are fully genetically encoded, and thus can be easily tuned and reconfigured through DNA manipulation. Empowered by directed evolution, this genetically encoded platform allowed for the rapid development of highly active biocatalysts for the enantioselective amination of primary, secondary, and tertiary aliphatic C–H bonds. Notably, some of these processes, such as the enantioconvergent tertiary C(sp^3)–H amination, have not been successfully implemented with small molecule catalysts. We anticipate that this biocatalytic platform can be further leveraged to tackle other challenges in enantioselective C–H functionalization and asymmetric catalysis in general.

Supplementary Material

Refer to Web version on PubMed Central for supplementary material.

Acknowledgements

The authors thank Ruijie K. Zhang, Kai Chen, David C. Miller, David K. Romney (Caltech) and Prof. Yiming Wang (University of Pittsburgh) for helpful discussions, Lawrence Henling for X-ray diffraction analysis, and Scott Virgil for assistance with chiral SFC analysis.

Funding: This work was supported by the NSF, Division of Molecular and Cellular Biosciences (grant MCB-1513007 for F.H.A. and CHE-1654122 for P.L.). Y.Y. thanks the National Institutes of Health for a postdoctoral fellowship (grant 1F32GM133126–01). Calculations were performed at the Center for Research Computing at the University of Pittsburgh. All data necessary to support the paper's conclusions are available in the main text and the Supplementary Information.

References

1. Gutekunst WR & Baran PS Chem. Soc. Rev. 40, 1976–1991, (2011). [PubMed: 21298176]
2. Hartwig JF & Larsen MA ACS Cent. Sci. 2, 281–292, (2016). [PubMed: 27294201]
3. Lu H & Zhang XP Chem. Soc. Rev. 40, 1899–1909, (2011). [PubMed: 21088785]
4. Saint-Denis TG, Zhu R-Y, Chen G, Wu Q-F & Yu J-Q Science 359, 759, (2018).
5. Davies HML & Manning JR Nature 451, 417, (2008). [PubMed: 18216847]
6. Quasdorf KW & Overman LE Nature 516, 181, (2014). [PubMed: 25503231]
7. Bhat V, Welin ER, Guo X & Stoltz BM Chem. Rev. 117, 4528–4561, (2017). [PubMed: 28164696]
8. Yang Y, Shi S-L, Niu D, Liu P & Buchwald SL Science 349, 62–66, (2015). [PubMed: 26138973]
9. Smalley AP, Cuthbertson JD & Gaunt MJ J. Am. Chem. Soc. 139, 1412–1415, (2017). [PubMed: 28064488]
10. Lewis JC, Coelho PS & Arnold FH Chem. Soc. Rev. 40, 2003–2021, (2011). [PubMed: 21079862]
11. Ortiz de Montellano PR Chem. Rev. 110, 932–948, (2010). [PubMed: 19769330]
12. Fasan R ACS Catal. 2, 647–666, (2012).

13. Coelho PS, Brustad EM, Kannan A & Arnold FH Science 339, 307–310, (2013). [PubMed: 23258409]
14. Kan SBJ, Lewis RD, Chen K & Arnold FH Science 354, 1048–1051, (2016). [PubMed: 27885032]
15. Key HM, Dydio P, Clark DS & Hartwig JF Nature 534, 534, (2016). [PubMed: 27296224]
16. Dydio P, Key HM, Hayashi H, Clark DS & Hartwig JF J. Am. Chem. Soc. 139, 1750–1753, (2017). [PubMed: 28080030]
17. Brandenberg OF, Fasan R & Arnold FH Curr Opin Biotechnol 47, 102–111, (2017). [PubMed: 28711855]
18. Singh R, Bordeaux M & Fasan R ACS Catal. 4, 546–552, (2014). [PubMed: 24634794]
19. Zhang RK et al. Nature 565, 67–72, (2019). [PubMed: 30568304]
20. McIntosh JA et al. Angew. Chem. Int. Ed. 52, 9309–9312, (2013).
21. Hyster TK, Farwell CC, Buller AR, McIntosh JA & Arnold FH J. Am. Chem. Soc. 136, 15505–15508, (2014).
22. Prier CK, Zhang RK, Buller AR, Brinkmann-Chen S & Arnold FH Nat. Chem. 9, 629, (2017). [PubMed: 28644476]
23. Kurokawa T, Kim M & Du Bois J Angew. Chem. Int. Ed. 48, 2777–2779, (2009).
24. Lu H, Jiang H, Wojtas L & Zhang XP Angew. Chem. Int. Ed. 49, 10192–10196, (2010).
25. Zalatan DN & Du Bois JJ Am. Chem. Soc. 130, 9220–9221, (2008).
26. Ichinose M et al. Angew. Chem. Int. Ed. 50, 9884–9887, (2011).
27. Roizen JL, Harvey ME & Du Bois J Acc. Chem. Res. 45, 911–922, (2012). [PubMed: 22546004]
28. Paradine SM & White MC J. Am. Chem. Soc. 134, 2036–2039, (2012). [PubMed: 22260649]
29. Paradine SM et al. Nat. Chem. 7, 987, (2015). [PubMed: 26587714]
30. Clark JR, Feng K, Sookezian A & White MC Nat. Chem. 10, 583–591, (2018). [PubMed: 29713037]
31. Li C et al. Angew. Chem. Int. Ed. 57, 16837–16841, (2018).
32. Lu H, Lang K, Jiang H, Wojtas L & Zhang XP Chem. Sci. 7, 6934–6939, (2016). [PubMed: 28138382]
33. Capdevila JH et al. J. Biol. Chem. 271, 22663–22671, (1996).
34. Chen K, Huang X, Kan SBJ, Zhang RK & Arnold FH Science 360, 71–75, (2018). [PubMed: 29622650]
35. Nagib DA Angew. Chem. Int. Ed. 56, 7354–7356, (2017).
36. Kainz QM et al. Science 351, 681–684, (2016). [PubMed: 26912852]
37. Wendlandt AE, Vangal P & Jacobsen EN Nature 556, 447–451, (2018). [PubMed: 29695848]
38. Zhang X et al. Science 363, 400–404, (2019). [PubMed: 30679372]
39. Hennessy ET, Liu RY, Iovan DA, Duncan RA & Betley TA Chem. Sci. 5, 1526–1532, (2014).
40. Singh R, Kolev JN, Sutera PA & Fasan R ACS Catal. 5, 1685–1691, (2015). [PubMed: 25954592]
41. Fandrick KR et al. J. Am. Chem. Soc. 133, 10332–10335, (2011).
42. Jacobs BP, Wolczanski PT, Jiang Q, Cundari TR & MacMillan SN J. Am. Chem. Soc. 139, 12145–12148, (2017).

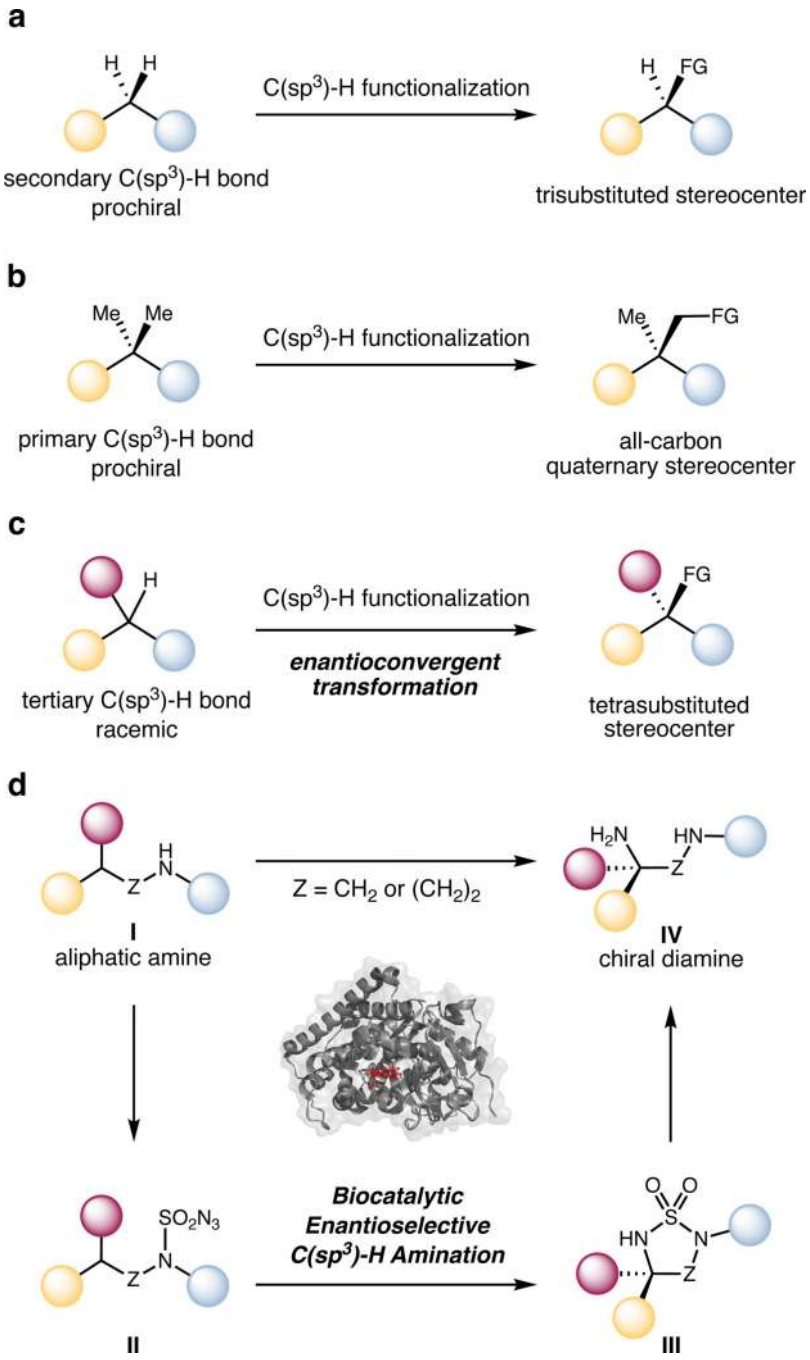

Fig. 1. Three major types of asymmetric C(sp^3)–H functionalization and biocatalytic C(sp^3)–H amination.

a, Enantioselective functionalization of secondary C(sp^3)–H bonds. **b**, Enantioselective functionalization of primary C(sp^3)–H bonds (i.e., desymmetrization of gem-dimethyl substituents). **c**, Enantioconvergent functionalization of tertiary C(sp^3)–H bonds. **d**, Proposed enzymatic synthesis of chiral diamines using C(sp^3)–H amination. FG = functional group.

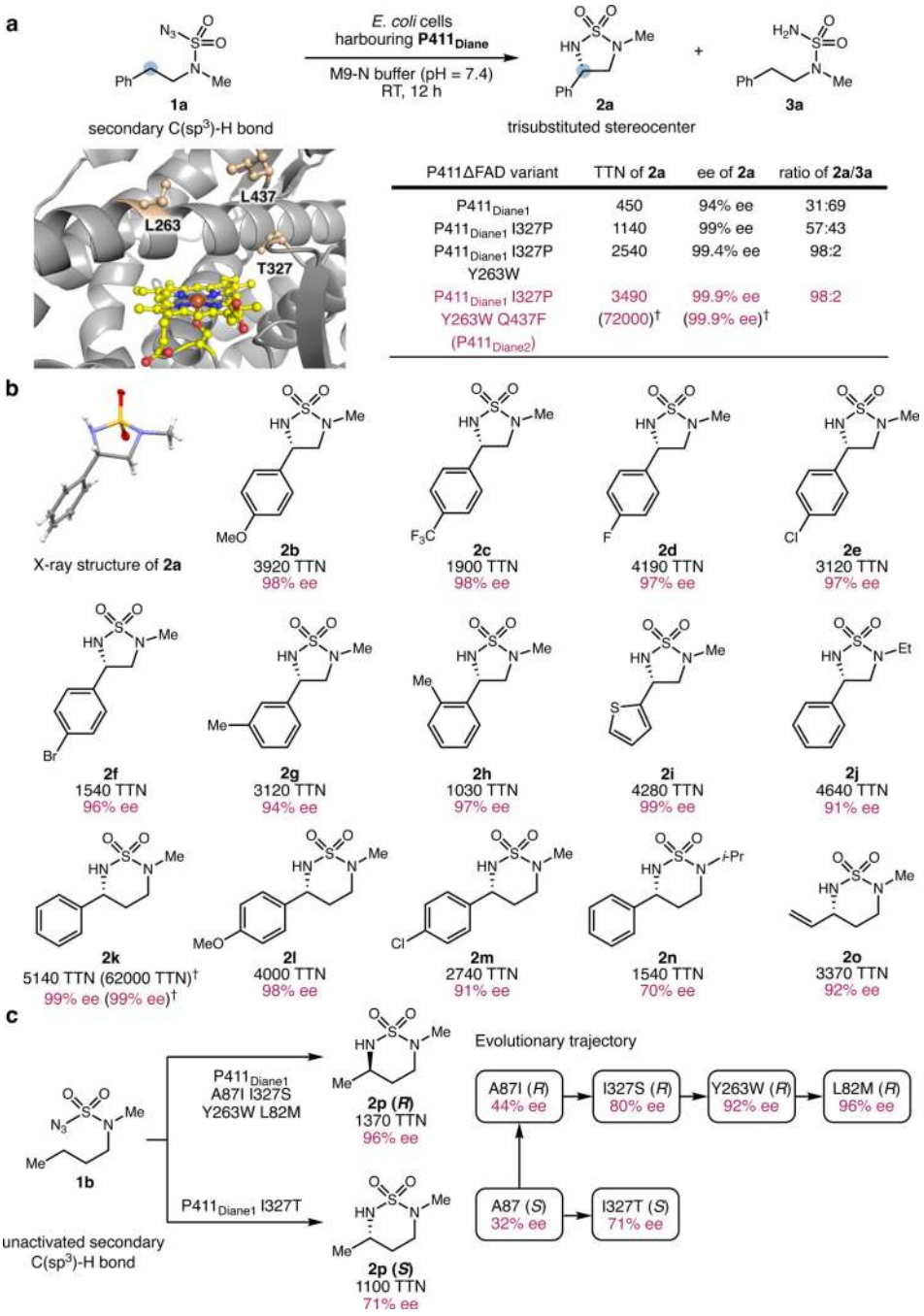

Fig. 2. Enantioselective amination of secondary C(sp^3)–H bonds.

a, Directed evolution of P411ΔFAD for the enantioselective synthesis of 1,2-diamines. Crystal structure of a variant closely related to P411$_{Diane1}$ is shown (Protein Data Bank ID: 5UCW); **b**, Substrate scope of 1,2-diamine and 1,3-diamine synthesis. **c**, Enantiodivergent amination of unactivated secondary C(sp^3)–H bonds to access either antipode of the diamine product. Experiments were performed using *E. coli* expressing cytochrome P411$_{Diane2}$ or P411$_{Diane1}$ (OD$_{600}$ = 30) with 10 mM substrate at room temperature under anaerobic conditions for 12–24 h. †High TTN experiments were performed using *E. coli* expressing

cytochrome $P411_{Diane2}$ or $P411_{Diane1}$ (OD_{600} = 1.9) with 20 mM substrate at room temperature under anaerobic conditions for 24 h.

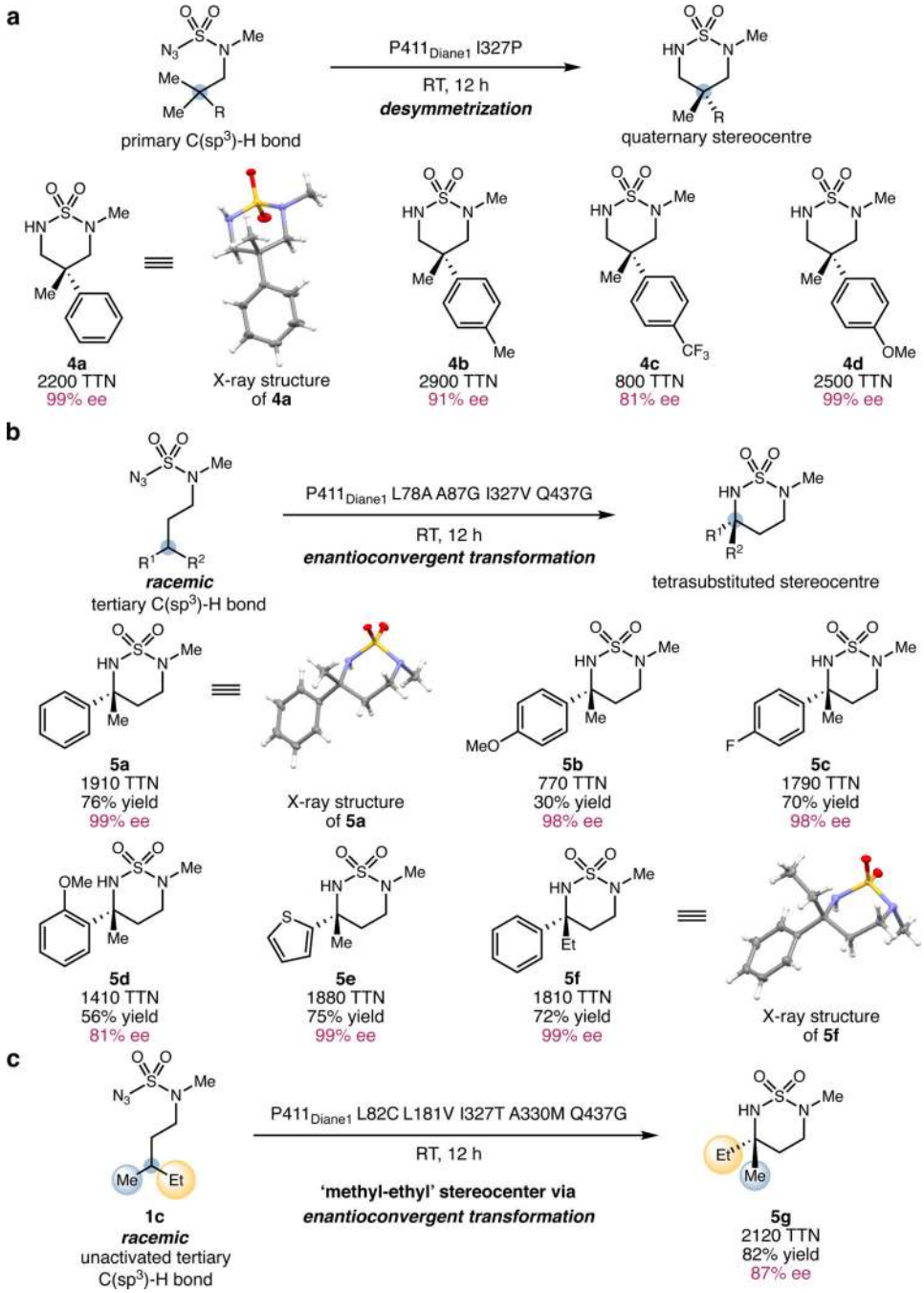

Fig. 3. Enantioselective amination of primary and tertiary C(sp^3)–H bonds.

a. asymmetric amination of primary C(sp^3)–H bonds (i.e., desymmetrization of geminal dimethyl substituents); **b**. Enantioconvergent amination of tertiary C(sp^3)–H bonds; **c**. Enantioconvergent construction of 'methyl-ethyl' stereocentre using tertiary C(sp^3)–H amination. Experiments were performed using *E. coli* expressing cytochrome P411$_{Diane1}$ I327P, P411$_{Diane1}$ L78A A87G I327V Q437G, and or P411$_{Diane1}$ L82C L181V I327T A330M Q437G (OD600 = 30–40) with 10 mM substrate at room temperature under anaerobic conditions for 12–24 h.

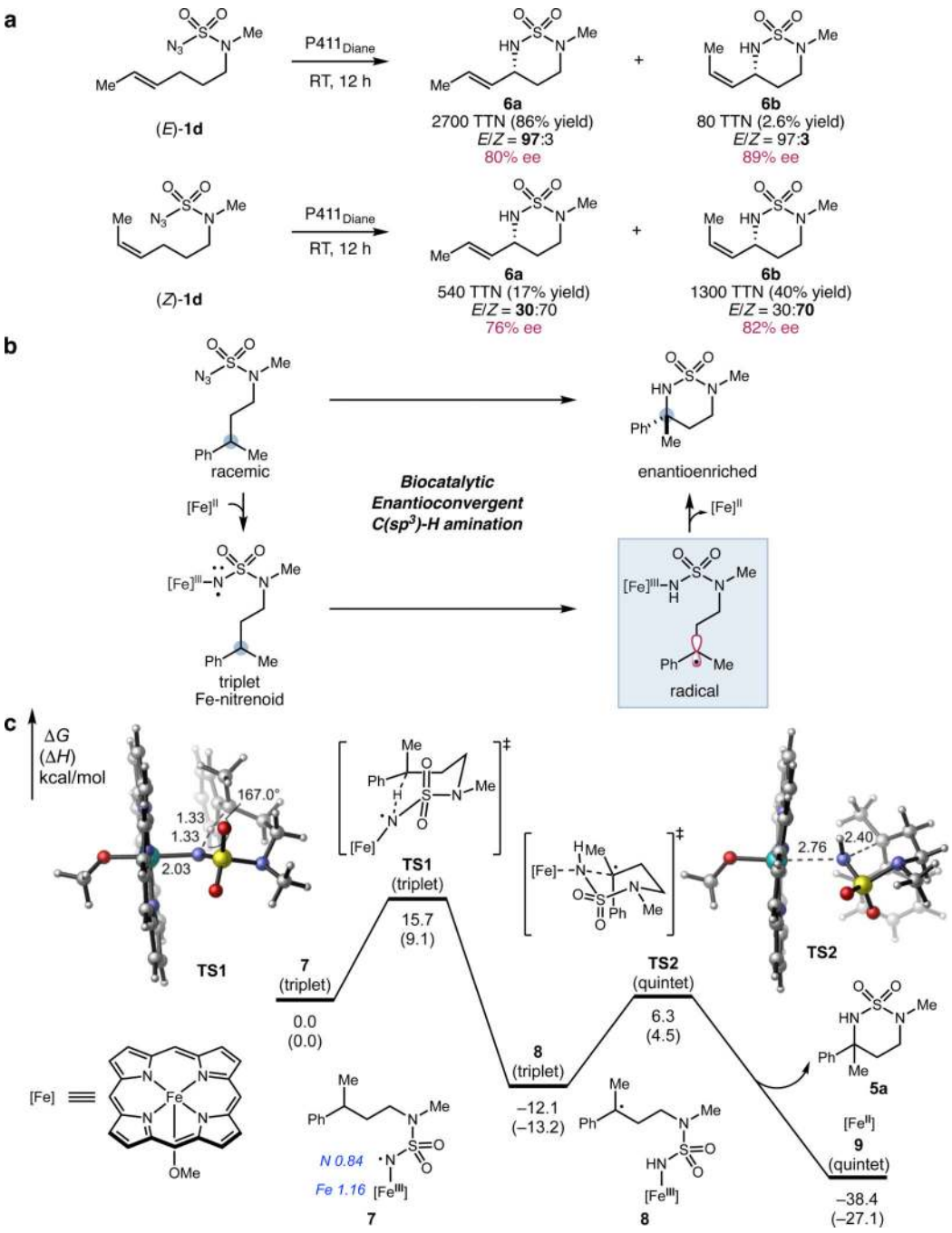

Fig. 4. Mechanistic and computational studies.

a. Scrambling of olefin stereochemistry during the allylic C(sp^3)–H amination of *(E)*- and (*Z*)-**1d** using P411 biocatalyst ($P411_{Diane1}$ I327P). **b**. Mechanistic proposal to account for the enantioconvergent amination of tertiary C(sp^3)–H bonds. **c**. Free energy profile of the iron porphyrin-catalysed C(sp^3)–H amination. Density functional theory (DFT) calculations were performed at the B3LYP-D3(BJ)/6–311+G(d,p)-LANL2TZ(f)/SMD(chlorobenzene)// B3LYP-D3(BJ)/6–31+G(d)-LANL2DZ level of theory. Triplet structures are shown in black

and quintet structures are shown in blue. Mulliken spin densities of Fe and N of the key iron nitrenoid 7 are shown in italic (blue).